Lamellar Metallo–Alkylphosphonates as Solid-State Phase-Change Materials

Oscar J. Almeida and Brian G. Dixon*

Cape Cod Research, Inc., 19 Research Road, East Falmouth, Massachusetts 02536

Received February 7, 1995. Revised Manuscript Received September 1, 1995[®]

A series of organo–metallophosphonates was synthesized that are solid-state phase-change materials (PCMs). These interesting composites have been shown to store latent heat as well as the best state of the art eutectic salt and organic PCMs, but as opposed to these traditional liquid-solid PCMs, the storage occurs totally in the solid state. In addition, the latent heat storage is reversible, and the phase transition temperature is adjustable over a wide temperature range.

Introduction

Solid-state phase-change materials (PCMs) are intriguing materials that have great potential in energy load leveling applications.[1–4] Although far less studied than their liquid to solid state PCM cousins, in fact they possess a number of superior properties. Inorganic PCMs, such as salt hydrates, tend to phase separate after a number of cycles. In addition they are corrosive materials. Organic PCMs, such as paraffins and neopentyl glycol, are extremely flammable. In all cases liquid to solid state PCMs must be contained, and thus the likelihood of leakage is an ever-present worry.

Probably the two most promising solid–solid latent heat systems are certain organic polymers, such as polyethylene,[5,6] and the so-called "layered perovskites".[6–9] Cross-linked polyethylene pellets have been shown to be practical latent heat storing materials but are useful only at elevated temperatures and are poor conductors of heat. The layered perovskites blend inorganic and organic chemistry to yield a composite in which there are alternating sheets, or layers, of organic and inorganic materials. These intriguing composites possess thermal conductivities an order of magnitude higher than typical organic phase-change materials (PCMs) and burn poorly.[6] The layered perovskites also have significant latent heats, and their phase transitions are totally reversible. Unfortunately, these materials contain amines, are a health hazard, and have unpleasant odors.

The research described herein was built upon the layered perovskite approach. It involved the synthesis of a series of metallo–alkylphosphonates that have been shown to possess a layered structure wherein the alkyl groups form pillars that are sandwiched between metallo–phosphorous backbone layers.[10] Compared to the perovskites, these new materials possess some very important advantages. The phosphorous moieties inhibit combustion, the compounds have no odor, and they are nonhazardous.

Metallo–organic phosphonates are a relatively new family of compounds that have been studied for their potential as shape-selective sorbents and catalysts or catalyst supports.[11–16] These intriguing microcrystalline materials have been shown to consist of alternating organic and inorganic layers as shown by the generic structure[17] in Scheme 1.

The layered structure of the total composite is shown in Scheme 1 and the location of the various components identified. The organic region is composed of long chain alkyl groups which form paraffin-like regions that will undergo the desired latent heat storage transformations. One end of each alkyl chain is covalently bound to a phosphorous atom which, in turn, is bound to a thin metal oxide layer that forms the structural backbone of the composite. By tailoring the type of alkyl groups attached to the phosphorous atoms, a systematic adjustment of the range of the phase change temperature transition can be achieved.

Experimental Section

All chemicals were purchased from the Aldrich Chemical Co., Milwaukee. In all cases the aqueous solutions were

---

[®] Abstract published in *Advance ACS Abstracts,* October 15, 1995.

(1) Garg, H. P.; Mullick, S. C.; Bhargava, A. K. *Solar Thermal Energy Storage*; D. Reidel: Boston, MA, 1985.

(2) Lane, G. A. *Solar Heat Storage: Latent Heat Material*; CRC Press: Boca Raton, FL, 1983.

(3) Benson, D. K.; Webb, J. D.; Burrows, R. W.; McFadden, J. D. O.; Christensen, C. *Materials Research for Passive Solar Systems: Solid-State Phase Change Materials*; SERI Report No. TR-255-1828; available from NTIC, Department of Commerce, Springfield, VA 22161, 1985.

(4) Piette, M. A.; Wyatt, E.; Harris, J. *Technology Assessment: Thermal Cool Storage in Commercial Buildings*, Lawrence Berkeley Laboratory Report No. LBL-25521; available from NTIC, Department of Commerce, Springfield, VA 22161, 1985.

(5) Salyer, I. O.; Davison, J. E. *J. Appl. Polym. Sci.* **1983**, *28*, 2903.

(6) Garg, H. P.; Mullick, S. C.; Bhargava, A. K. *Solar Thermal Energy Storage*; D. Reidel: Boston, MA, 1985.

(7) Busico, V.; Carfagna, C.; Salerno, V.; Vacatello, M. *Sol. Energy* **1980**, *24*, 575.

(8) Busico, V.; Corradini, P.; Migliaresi, C.; Nicholais, L. *J. Appl. Polym. Sci.* **1980**, *25*, 2857.

(9) Nicholais, A. A.; Busico, V.; Migliaresi, C. *Appl. Energy* **1980**, *6*, 353.

(10) Cao, G.; Hong, H.; Mallouk, T. E. *Acc. Chem. Res.* **1992**, *25*, 420.

(11) Yamanaka, S.; Sakamoto, K.; Hattori, M. *J. Phys. Chem.* **1984**, *88*, 2067.

(12) Cao, G.; Lee, H.; Lynch, V. M.; Mallouk, T. E. *Inorg. Chem.* **1988**, *27*, 2781.

(13) Johnson, J. W.; Jacobson, A. J.; Butler, W. M.; Rosenthal, S. E.; Brody, J. F.; Lewandowski, J. T. *J. Am. Chem. Soc.* **1989**, *111*, 381.

(14) Dines, M. B.; DiGiacomo, P. M. *Inorg. Chem.* **1981**, *20*, 92.

(15) Dines, M. B.; Cooksey, R. E.; Griffith, P. C.; Lane, R. H. *Inorg. Chem.* **1983**, *22*, 1003.

(16) Dines, M. B.; Griffith, P. C. *Inorg. Chem.* **1983**, *22*, 567.

(17) Bujoli, B.; Palvadeau, P.; Rouxel, J. *Chem. Mater.* **1990**, *2*, 582 and references therein.

0897-4756/95/2807-2039$09.00/0

Scheme 1

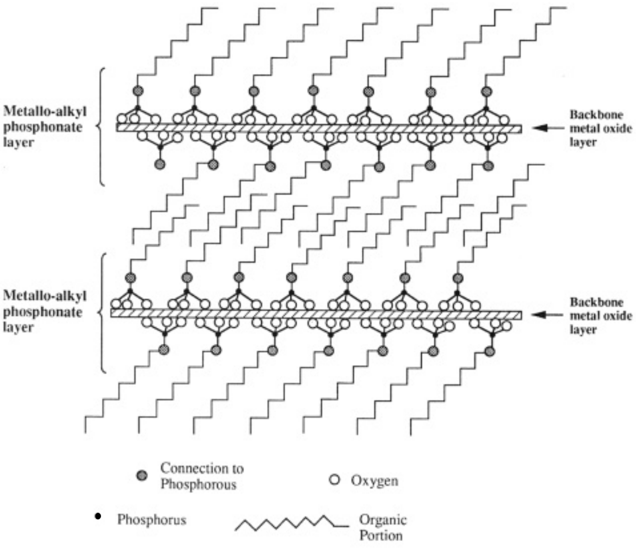

prepared using deionized water. IR analyses were obtained on a Perkin-Elmer Model 1600 FTIR equipped with MIR, diffuse reflectance, and fixed angle specular attachments. Thermal analyses were performed on a Perkin-Elmer Model Delta Series DSC7 equipped with a Perkin-Elmer Model 3700 Data Station, a Perkin-Elmer TAC 7/3 Instrument Controller, and a Perkin-Elmer Graphics Plotter 2, at a scanning rate of 10 or 20 °C/min. All heating and cooling curves were normalized to a sample weight of 1 mg.

Exemplary Arbuzov Synthesis.[13] **Dimethoxy *n*-hexadecyl phosphonate**: Trimethyl phosphite (50 mL, 0.42 mol) and *n*-hexadecyl bromide (130 mL, 0.42 mol) were mixed together in a 500 mL boiling flask without solvent and heated to reflux for 48 h. The yellow orange reaction mixture was then purified using liquid chromatography (hexane/ethyl acetate) which yielded a yellow liquid; yield 72%. IR peaks at 2925 and 2854 (CH), 1466 ($-CH_2-$), 1379 ($-CH_3$), 1249 (P=O), ~1025 (P–O, ether), 723 (extended $-CH_2-$) cm^{-1}. Other phosphonate esters were obtained similarly, by simply substituting the corresponding number of moles of the alkyl bromide of the desired chain length.

Sodium Salt Synthesis. In a typical reaction, 0.100 mol of the sodium metal was added to a 500 mL round-bottom flask containing 300 mL of dried toluene, and the mixture was stirred. The toluene was heated to a gentle reflux and stirred. Dibutyl phosphite (0.100 mol) was added dropwise over a period of a half-hour. Complete reaction of the sodium with the phosphite produced a clear, hazy solution. The alkyl halide (0.100 mol) was added dropwise over 45 min. The reaction was refluxed for 6 h and was accompanied by the formation of a white precipitate. After being cooled, the solids were filtered. The filtrate was washed with three 100 mL portions of a cold, weak sodium chloride solution, dried over magnesium sulfate, and filtered. The solvent was removed in vacuo, leaving behind the alkyl phosphonate.

Phosphonic Acid Synthesis.[14] In a typical reaction, the alkyl phosphonate diester, obtained from either the Arbuzov or sodium salt reaction sequence, was dissolved in 100 mL of acetic acid, heated, and reacted with hydrogen bromide in acetic acid using a 100% excess of HBr. The butyl bromide was continuously distilled off, and HBr was added until butyl bromide production stopped. The reaction mixture was cooled and poured into 300 mL of cold 10% HCl solution while vigorously stirring. The solid product was filtered, washed with hexane and dried under vacuum at ~25 °C. IR spectrum of the C_{20} phosphonic acid: 3300–2500 (v br, OH), 2916 (CH), 1472 ($-CH_2-$), 1390 ($-CH_3$), 1225–952 ($-P-O-$), 717 (extended $-CH_2-$) cm^{-1}.

Phosphonic Acid Salt Syntheses. Zn, Mg.[12,18] In a typical reaction, 0.02 mol of the alkylphosphonic acid of choice was dissolved in 400 mL of 75% methanol/water solution and heated. After a clear solution was achieved, a mixture of the corresponding metal salt in 80 mL of water was added. The stoichiometry of the reaction was based upon a 1:1 metal ion to $R-PO(OH)_2$ ratio. A white precipitate formed instantly. The mixture was then stirred until it cooled to room temperature, and sufficient NaOH was added to bring the mixture to a pH of 2. The solid product was filtered, washed with water and dried under vacuum at ~25 °C. Elemental analyses for C and H agreed with the formula $M(O_3PR){\cdot}H_2O$, as expected from the literature precedent.[12] By way of example for $Zn(O_3PC_{18}H_{37})$: obtained 51.23% C, 9.13% H, 7.30% P. Expected: 51.14% C, 9.23% H, 7.34% P. For $Mg(O_3PC_{18}H_{37})$: obtained 56.78% C, 10.12% H, 8.10% P. Expected: 56.64% C, 10.23% H, 8.13% P. IR peaks: (Zn) 3500–3000 (v br, OH), 2915, 2847 (CH), 1466 ($-CH_2-$), 1375 ($-CH_3$), 1147–925 ($-P-O-$), 720 (extended $-CH_2-$), 580 ($-ZnO-$) cm^{-1}. (Mg) 3500–3000 (v br, OH), 2916, 2849 (CH), 1472 ($-CH_2-$), 1390 ($-CH_3$), 1225–952 ($-P-O-$), 717 (extended $-CH_2-$), 566 ($-MgO-$) cm^{-1}.

Scheme 2

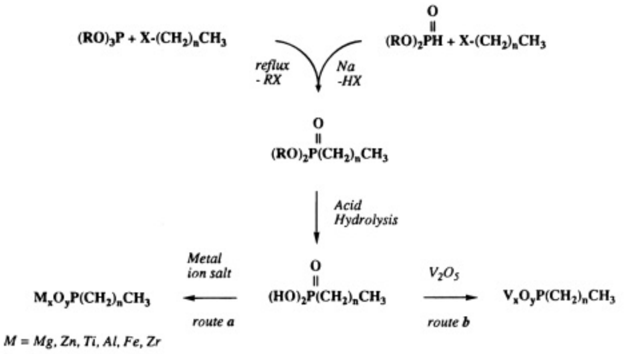

Vanadium.[13,18] Vanadyl *n*-hexylphosphonate: finely ground V_2O_5 (0.273 g, 1.5 mmol) was added to a solution of *n*-hexylphosphonic acid, $(C_6H_{13})PO(OH)_2$ (0.548 g, 3.3 mmol), in 30 mL of ethyl alcohol plus 0.9 mL of 1 M HCl (0.05 mol of H_2O, 0.9 mmol of HCl). While heating at reflux for 6 h, the mixture turned from the original orange color to a green and finally a blue as the reaction proceeded. The product was isolated by filtration, washed with ether, dried for 3 h at 110 °C under high vacuum, and ground to a fine powder. Elemental analyses agreed with the formula $VO(C_6H_{13}PO_3){\cdot}H_2O{\cdot}CH_3CH_2OH$ as expected from literature precedent.[13] Obtained 35.64% C, 7.62% H, 11.31% P. Expected: 35.42% C, 7.75% H, 11.44% P. IR peaks: 2920, 2850 (CH), 1469 (CH_2), 100–960 (P–O, V–O) 910 (VO) 800 (VO) and 715 (extended CH_2), 423, 460 (V–O–V) cm^{-1}.

Results and Discussion

Syntheses. The basic synthetic routes to the layered metallo-alkyl phosphonates are shown in Scheme 2. In all cases, the first two steps involved the synthesis of the desired alkylphosphonic acid. Two synthetic routes to the phosphonic acids were evaluated, both of which yielded the desired products. Except for the vanadium complexes, the formation of the final layered composites involved simply reacting the desired alkyl phosphonic acid with a suitable metal ion salt to yield the final product (route **a**). In the case of vanadium, the reaction was carried out in a heterogeneous fashion by stirring vanadium pentoxide powder with a solution of the alkylphosphonic acid in ethanol (route **b**). In the latter case, the reaction is easily followed spectrophotometrically by the appearance of a beautiful powder blue color

---

(18) For X-ray structures of these compositions: see ref 10 and references therein.

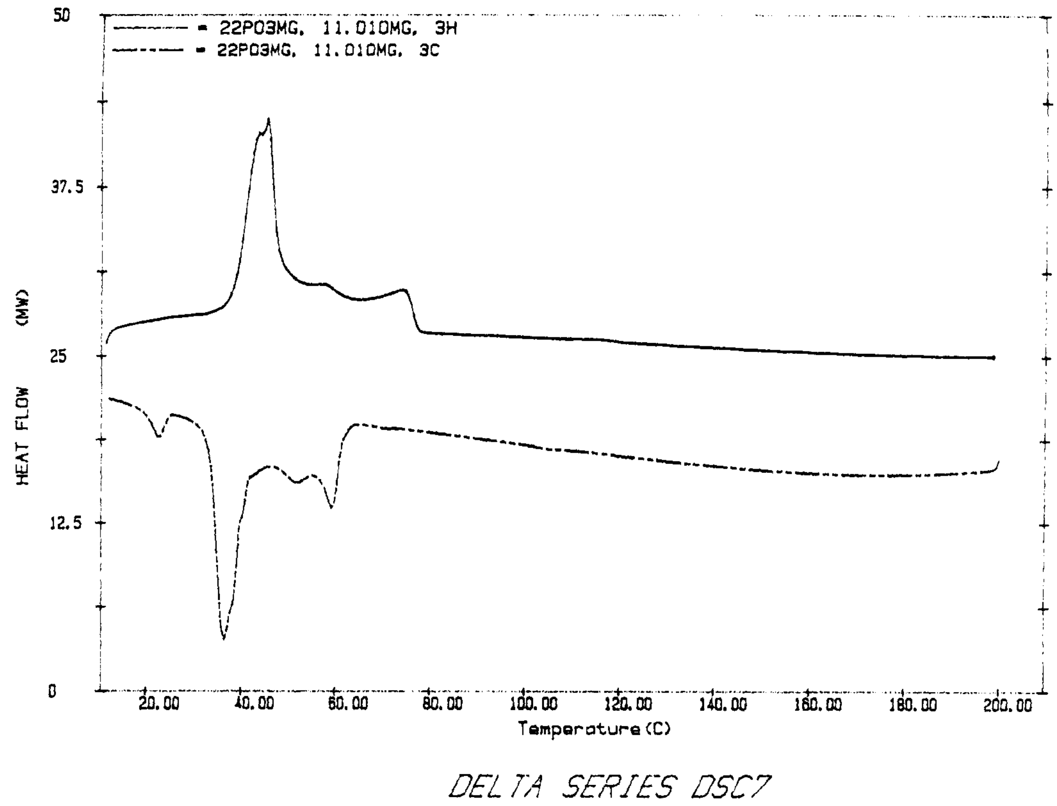

Figure 1. Differential scanning calorimetry (DSC) of $Zn_xO_yP(CH_2)_{21}CH_3$.

that is characteristic of the V^{4+} ion. The series of compounds made and evaluated included

$Zn[O_3P(CH_2)_nCH_3]$
where $n = 1, 2, 14, 15, 16, 17, 18, 20, 22$

$Mg[O_3P(CH_2)_nCH_3]$
where $n = 14, 15, 16, 17, 18, 20, 22$

$VO[O_3P(CH_2)_nCH_3]$
where $n = 14, 15, 16, 17, 18, 20, 22$

The first two entries of the zinc series, carbon chain lengths C_1 and C_2, were run as controls to demonstrate the requirement for long alkyl chains for storing heat.

Thermal Properties. All of the complexes demonstrated the capability to reversibly store heat, and many of the latent heat values were quite high. Early on in the research effort, it became clear that the newly synthesized materials were indeed capable of reversibly storing significant amounts of heat, over a wide temperature range, and that this range could be adjusted in a systematic fashion.

The calorimetry plot shown in Figure 1 typifies the best of the experimental results. This differential scanning calorimetry (DSC) plot, run on a magnesium-based organophosphonate of alkyl chain length C_{22}, had an outstanding latent heat value of 212 J/g. The dramatic increase in latent heat storage is consistent with a significant increase in molecular order, as has been previously observed in perovskite–alkylamine intercalates.[7,8]

Other notable points within this graph include the broad temperature range of heat absorption and emission, the attractive temperature range within which the transitions occur, and the reproducibility of the event.

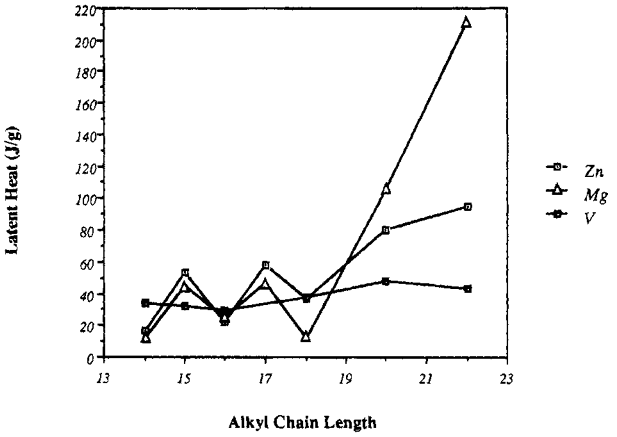

Figure 2. Latent heat (cooling) as a function of alkyl chain length.

That is, this plot represents the third iteration of the DSC scanning process. By way of comparison, the classical liquid–solid PCM materials, paraffin and Glauber's salt, possess latent heats of ~230 and ~240 J/g, respectively. However, the totally solid-state nature of the phase change of the new metallooxy–alkylphosphonate materials represents a significant step forward in the state of the art. This is a critical point in that all of the observed transitions were truly solid-state changes, and no liquefaction was observed. This fact was ascertained by simply heating up samples of the various compounds and observing their response. In some cases, a change from opaque to translucent was observed which is consistent with, but certainly not proof of, a thermally induced phase change. Not unexpectedly, the longer C_{20} and C_{22} alkyl chain length composites yielded superior latent heats, as demonstrated by the latent heat values for the zinc, magnesium, and vanadium series shown in Figure 2 (the

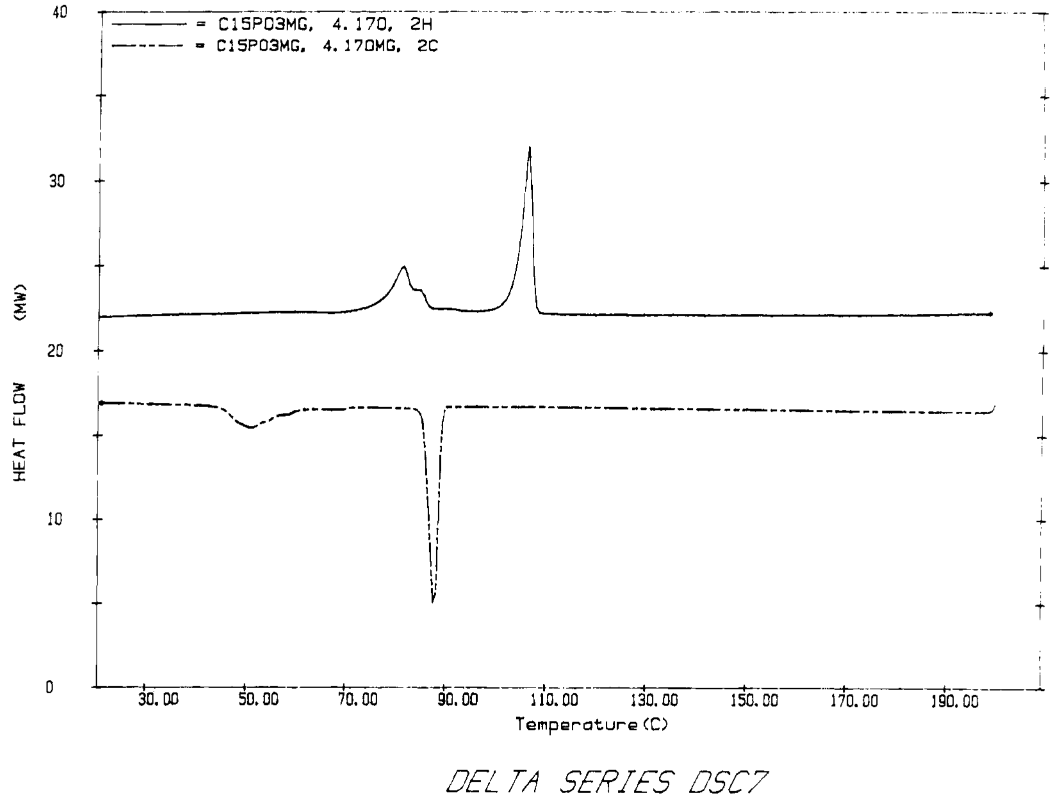

Figure 3. Differential scanning calorimetry (DSC) of $Mg_xO_yP(CH_2)_{14}CH_3$.

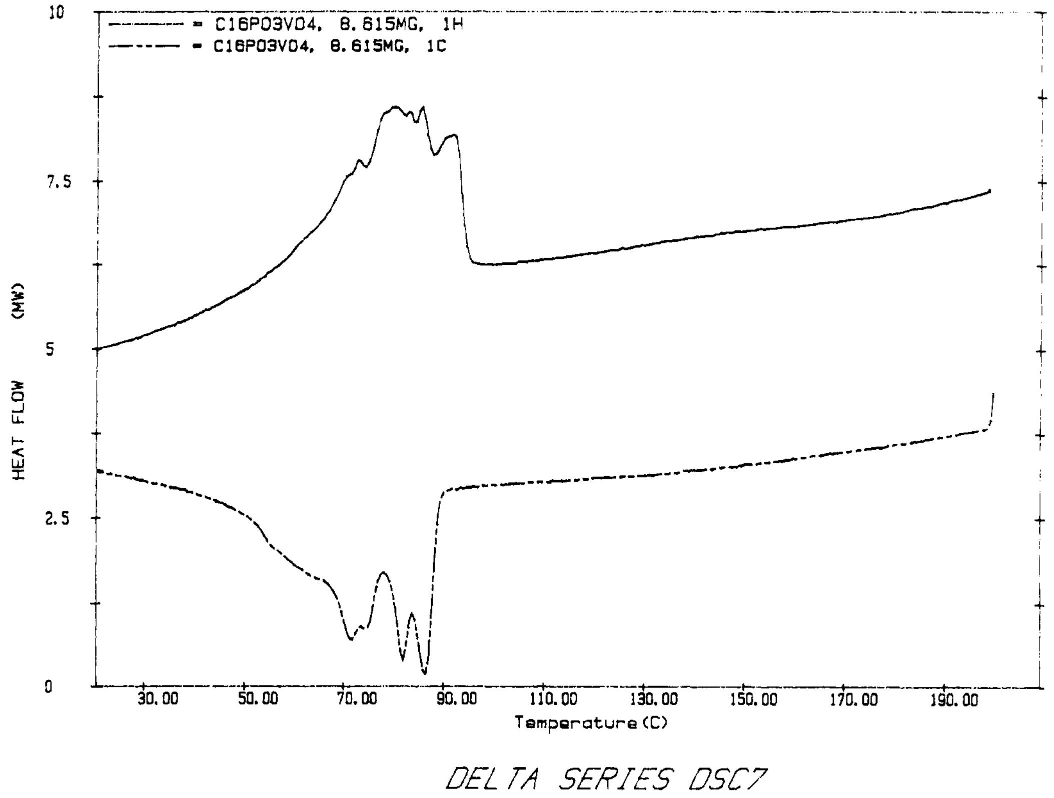

Figure 4. Differential scanning calorimetry (DSC) of $V_xO_yP(CH_2)_{15}CH_3$.

points represent the averages of three separate runs). A striking result is the odd–even effect observed for Zn and Mg, which is clearly evident in this graph. The odd-numbered chain lengths, C_{15} and C_{17}, have significantly higher latent heats than the C_{14}, C_{16}, and C_{18} composites that surround them on the plot. This type of effect is well-known for other properties of simple alkanes.

An unexpected result, also strikingly apparent in Figure 2, was the effect of the metal ion type that comprised the oxide layer. The latent heats of the vanadium series were remarkably insensitive to the length of the alkyl chains, and no odd–even effect was observed. One obvious difference between vanadium and the other two metals is the oxidation state of the

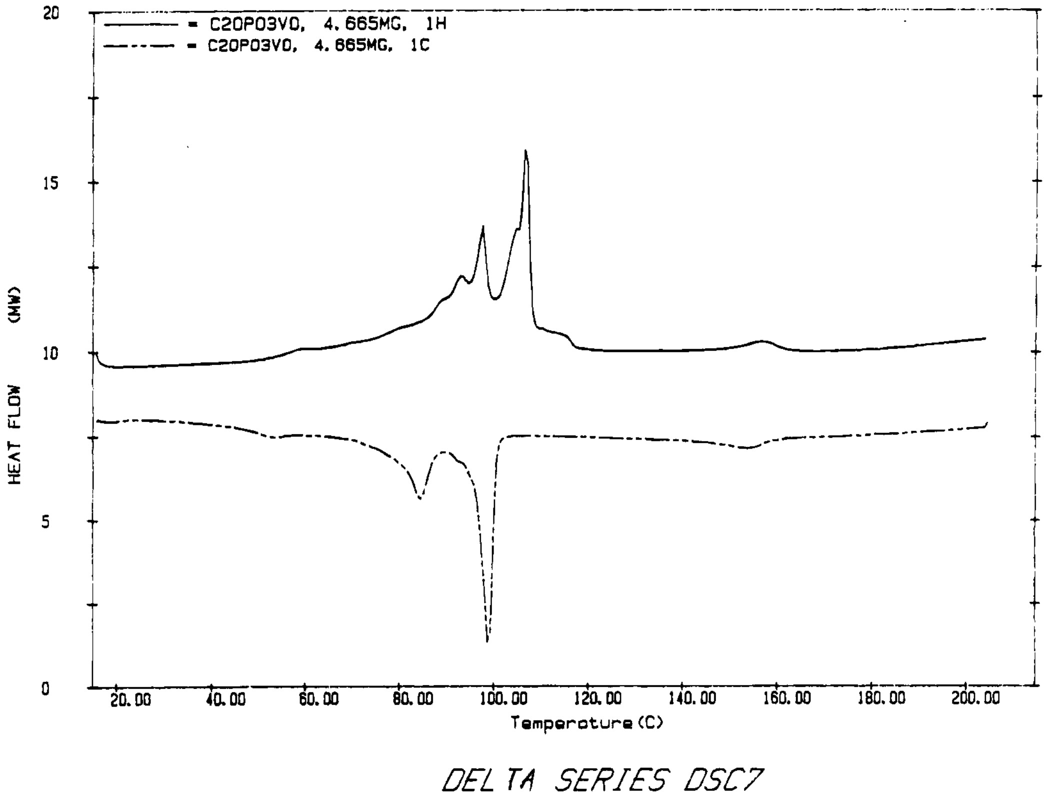

Figure 5. Differential scanning calorimetry (DSC) of $V_xO_yP(CH_2)_{19}CH_3$.

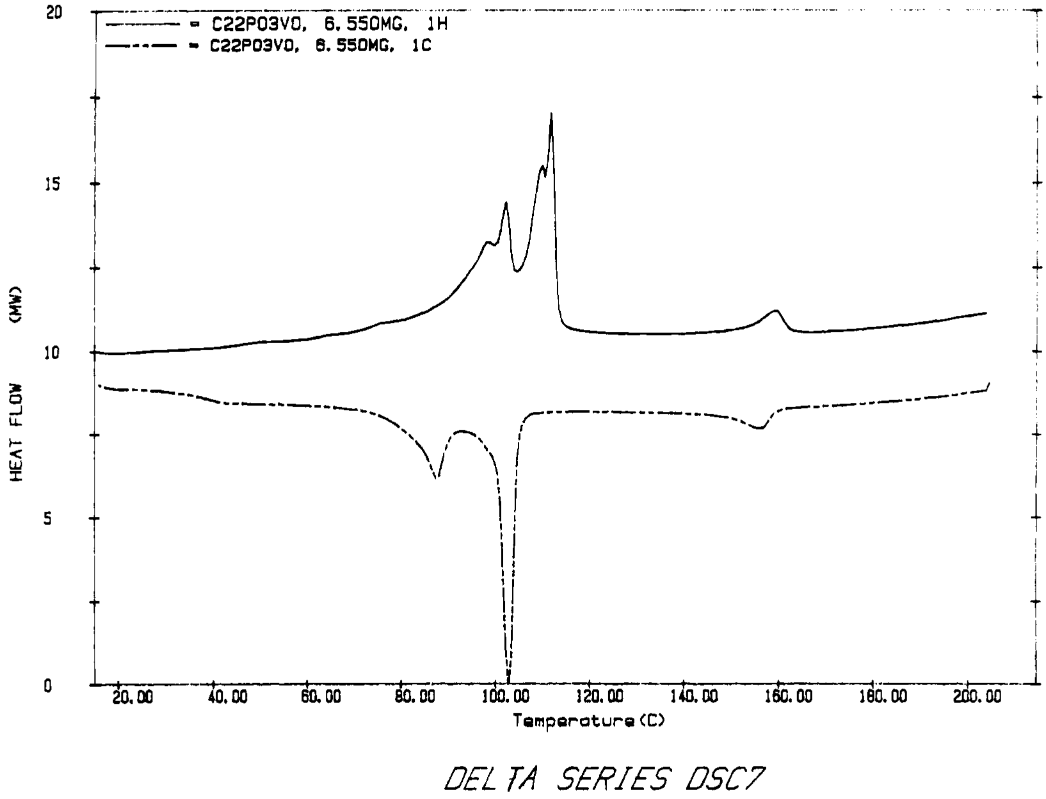

Figure 6. Differential scanning calorimetry (DSC) of $V_xO_yP(CH_2)_{21}CH_3$.

respective metal ions. Possibly the +4 oxidation state of vanadium has a significant effect upon composite structure and thus the resultant thermal properties. Studies with other metal ions are currently under way to evaluate the effect of the metal oxidation state. The zinc and magnesium series gave results that were very sensitive to chain length, but the increase in latent heats increased much more rapidly for the magnesium than the zinc at the longer chain lengths. The reasons for this trend are also unclear, but under investigation in our laboratories.

The latent heat of fusion is a critical parameter for heat-storage materials, and the latent heats measured (up to 212 J/g) are equal to the best values obtained with state-of-the-art eutectic PCMs, as well as the perovskites.[1-9]

The investigation discovered that metallo–alkylphosphonates store significant amounts of heat reversibly at a number of different temperatures and that the storage temperature depended on chemical structure. This is unlike ice or eutectic materials where the system must be designed around the melting point. Transition temperatures between 10 and 175 °C were obtained. In contrast to classical PCMs, which give sharp and narrow transition temperatures, broad temperature range transitions were the norm for most of the new solid-state materials. This fact is demonstrated by the DSC scans of Figure 1, as well as Figures 3–6. Most of the DSC scans were iterated three times and were found to be reversible. Figure 3 represents a typical DSC scan for the Mg_{15} phosphonate.

There was also a pronounced peak broadening observed with the Zn_{15}, Mg_{15}, and Zn_{22} samples with each successive cycle. Most likely, this broadening was due to the formation of less organized (kinetic) states with succeeding cycles. However, the V_{16} sample (a typical scan shown by Figures 4) did not show significant broadening.

This was an interesting and unexpected result that suggests a fundamental difference in thermodynamic character between the vanadium composites and those based upon the other metals, as was alluded to above in Figure 2. It is possible that this difference was due to the different synthetic approaches to the layered structures or to the different metallic oxidation states, but the suggestion is that the underlying chemistry is quite rich and, as yet, relatively unexplored.

Another interesting observation was that the vanadium complexes all exhibited a reproducible fine structure in their peak transitions (compare Figures 4–6). In addition, the similarity of the fine structures in the V_{20} (Figure 5) and V_{22} (Figure 6) scans is unmistakable.

Yet another intriguing fact is that the temperature differential between the heating and cooling peaks varied significantly depending upon a composite's identity. While the Zn and Mg gave big separations, the V samples gave heating and cooling scans that almost overlapped. Our studies with these interesting composites are continuing.

Acknowledgment. The financial support of the Department of Energy under Grant No. DE-FG02-90ER80895 is gratefully acknowledged.

CM950059I